Quantitative, super-resolution localization of small RNAs with sRNA-PAINT

Kun Huang [1,2], Feray Demirci [3], Blake C. Meyers [4,5*], Jeffrey L. Caplan [1,2*]

[1] Department of Plant and Soil Sciences, University of Delaware, Newark, DE 19716, USA

[2] Bio-Imaging Center, Delaware Biotechnology Institute, University of Delaware, Newark, DE 19716, USA

[3] FiDoSoft Software Consulting, Redmond, WA, 98053, USA

[4] Donald Danforth Plant Science Center, 975 North Warson Road, St. Louis, Missouri 63132, USA

[5] University of Missouri – Columbia, Division of Plant Sciences, 52 Agriculture Lab, Columbia, MO 65211

* To whom correspondence should be addressed: Jeffrey L. Caplan; Tel: (302) 831-3403; Fax: (302) 831-4841; Email: jcaplan@udel.edu

Correspondence may also be addressed to: Blake C. Meyers; Tel: (314) 587-1422; Email: bmeyers@danforthcenter.org

Keywords

Small RNA, RNA detection, DNA-PAINT, *in situ* hybridization, super-resolution, single molecule, microscopy, maize anther, quantification

Abstract

Small RNAs are non-coding RNAs that play important roles in the life of both animals and plants. They are 21- to 24-nt in length and around 10 nm in size. Their small size and high diversity has made it challenging to develop methods that have sufficient resolution and specificity to multiplex and quantify. We created a method for the detection of small RNA with nanometer resolution by combining the super-resolution method, DNA-based points accumulation in nanoscale topography (DNA-PAINT), and the specificity of locked nucleic acid (LNA) probes for the *in situ* detection of multiple small RNAs. The method relies on designing probes to target small RNAs that combine the DNA oligos for PAINT with the LNA-containing oligos for hybridization; therefore, we developed an online tool called "Vetting & Analysis of RNA for *in situ* Hybridization probes" (VARNISH) for probe design. Our method utilizes advances in DNA-PAINT methodologies, including qPAINT for quantification and Exchange-PAINT for multiplexing. We demonstrated these capabilities or sRNA-PAINT by detecting and quantifying small RNAs in different cell layers of early developmental stage maize anther that are important for male sexual reproduction.

Introduction

In plants, 21- to 24-nucleotide (nt), non-coding small RNAs (sRNAs) regulate many important biological processes [1]. Plant and animal genomes encode various sRNAs that can be divided in two major categories: microRNAs (miRNAs) and small interfering RNAs (siRNAs) [2]. miRNAs derived from long, hairpin precursor RNAs processed by precise cleavage, yielding mature miRNAs which influence gene transcript levels and translation [3]. Plant siRNAs also derive from long precursors that are made double-stranded by RNA-dependent RNA polymerases (RDRPs), are processed to siRNAs, and also regulate gene transcript levels, through post-transcriptional silencing and epigenetically via RNA-directed DNA methylation (RdDM) [4]. Some plant miRNAs trigger phased, secondary siRNAs (phasiRNAs), which are either 21 or 24 nt in length[5-7]. Anthers, the plant male reproductive organ, are a particularly rich source of miRNAs and phasiRNAs, particularly in grasses like maize [7]; during the meiotic stage, they are composed of cell layers that include the epidermis, endothecium, middle, and tapetum, that all surround the pollen mother cells. In maize anthers, the abundance and distribution of miRNAs and phasiRNAs varies in different cell layers [7], and our interest in the spatial organization and concentration of these sRNAs, particularly at the subcellular level, provided us a strong motivation to develop new methods for fluorescent detection.

33 sRNAs are always on the move [8], moving within and between organelles, from cell-to-cell, long distances
34 within an organism, and there is increasing interest in their functions across organismal boundaries, in
35 plant-pathogen interactions. For example, within a cell, sRNAs move between the nucleus and
36 cytoplasm, bind Argonaute (AGO) proteins, Dicing bodies (D-bodies), Cajal bodies (CBs), and may be
37 polysome-associated or found with organelles such as the endoplasmic reticulum [9-12]. Intercellular
38 movement of sRNAs, presumably via plasmodesmata in plants, regulates tissue and organ development
39 by silencing and regulating developmentally important genes [13]. Systemic translocation of sRNAs has
40 been demonstrated by epigenetic silencing across graft junctions and sRNA profiling of vasculature [8, 14].
41 Remarkably, sRNAs also move between organisms at host-pathogen interfaces [15]. Pathogens, including
42 parasitic plants, regulate host defense responses via miRNAs and *trans*-species sRNAs, and *vice versa* [16].
43 In animals, extracellular vesicles (EVs) transport miRNAs from cell-to-cell and over long-distances [17].
44 Plant EVs are populated with miRNAs and fragments as small as 10 to 17 nt, the so-called tiny RNAs [2]. All
45 of these sRNAs vary in abundance from low to extremely high in abundance, as measured from
46 sequencing data, which typically utilizes gram quantities of plant tissue, substantially limiting spatial
47 analyses. And at the subcellular level, the localizations of these RNAs are not well-characterized. Thus,
48 future approaches to sRNA characterization will require nanometer resolution, high specificity, and both
49 multiplexing and quantitative capabilities.
50
51 For *in situ* hybridization of sRNAs, the use of locked nucleic acid (LNA) oligonucleotide probes has shown
52 specificity and high fidelity [18]. However, colorimetric and even fluorescent localization of sRNAs using
53 LNA-based methods are able to resolve only tissue-level localization patterns. Because of the limits of
54 light diffraction, lens-based microscopy cannot resolve spots below ~200 nm in diameter and 400 to 700
55 nm in axial length [19]. New techniques known as Photoactivated Localization Microscopy (PALM),
56 Structured Illumination microscopy (SIM), direct Stochastic Optical Reconstruction Microscopy
57 (dSTORM), and Points Accumulation for Imaging in Nanoscale Topography (PAINT) have been used to
58 drive microscopic detection beyond the diffraction limit, yielding so-called “super-resolution”
59 microspopy [19]. We have previously demonstrated an sRNA-FISH method combined with SIM and
60 dSTORM [20]. However, PALM and dSTORM utilize the blinking property of fluorescent dyes and rely on
61 specific excitation and buffer conditions to achieve proper imaging [21]. Photoswitching of the dye
62 molecule is hard to predict, which made absolute quantification difficult using these methods. The
63 number of dyes with the appropriate photoswitching properties within the visible spectrum is also a
64 limiting factor for multiplexed detection [21]. DNA-PAINT decouples the blinking events from dye

65 photophysics, using the binding and dwelling kinetics of a short dye-labeled oligonucleotide "imager
66 strand" to localize target-specific "docking strands" [22, 23]. The docking strand in DNA-PAINT is linked to an
67 antibody for single-molecule protein detection, with imager strands introduced by perfusion, one
68 imager strand at a time, each specific to a given docking strand and protein. After the image is acquired,
69 the imager strand is washed off and then the next imager strand is introduced [21]. As a result, a single dye
70 can be linked to different imager strands and applied for detection of numerous protein targets via use
71 of different imager strand-docking strand combinations. This multiplexing technique, known as
72 "Exchange-PAINT" has been used to *in situ* imaging of protein targets, such as microtubules and
73 mitochondria [23], and *in vitro* profiling of miRNAs to a synthetic DNA origami [24].
74
75 To achieve subcellular, nanometer resolution imaging for the localization and analysis of sRNAs, we
76 created a detection method called sRNA-PAINT. This method combines the high resolution and precise
77 quantification of DNA-PAINT with the efficiency and specificity of LNA-based *in situ* hybridization. We
78 created a probe design tool for our method and show that these sRNA-PAINT probes can used for robust
79 sRNA detection. And, we demonstrate that it can be combined with qPAINT to localize and quantify
80 distinct sRNAs in fixed biological sample and Exchange-PAINT for multiplexed target detection.
81
82 **Results**
83 *sRNA-PAINT probe design*
84 Most sRNA backbones are between 21 to 24 nt in length. To perform sRNA-PAINT, we designed a probe
85 that is composed of three sequences: the probe backbone sequence with LNA bases, the DNA-PAINT
86 docking strand sequence, and a linker sequence that connects those two (shown in Fig. 1). The probe
87 design is the most critical step of the sRNA-PAINT method, and therefore, we created an online tool
88 called VARNISH (Vetting & Analysis of RNA for *in situ* Hybridization probes) for automated design of
89 sRNA-PAINT probes (https://wasabi.ddpsc.org/~apps/varnish/). The tool requires the input of a target
90 sRNA sequence and the hybridization parameters (defaults provided), including sodium (50 mM) and
91 temperature (25°C). VARNISH first will reverse complement the sRNA sequence and will then chose
92 between 19-22 nt of the sequence such that the melting point temperature (T_m) is lower than 60°C, with
93 preference for lower T_m values for the longest sequence length. The melting temperature is calculated
94 by calling the "Analyze" function from the IDT web application program interface (API)
95 (https://www.idtdna.com/AnalyzerService/AnalyzerService.asmx). The final sequence is the probe
96 backbone (Fig. 1, cyan). Next, LNA bases and a linker sequence are introduced to the selected probe

97 backbone by VARNISH. The default linker sequence is “tattcgt”, which has no match to the sRNA
98 sequences in miRbase, but this can be changed to any custom linker sequence. VARNISH introduces
99 between five and nine LNA bases (default is eight) and it avoids stretches of more than four LNA bases
100 and three or more Gs or Cs. The algorithm exhausts all the possible combinations of the positions for
101 LNA bases, and it calculates the approximate T_m using previously estimated T_m values for different LNAs
102 [25]. Next, VARNISH takes the top 200 probe backbone candidates with the highest TM T_m and it calculates
103 the exact T_m using the IDT web API. The last step is adding the DNA-PAINT docking strand. In the
104 VARNISH tool, the docking strand can be either chosen from a drop down menu containing the 13
105 previously used docking strands [23] or the sequence can be entered manually in the VARNISH tool. The
106 software will conduct a homo-dimer and secondary structure analysis from all or a subset of the 13
107 provided docking strands in combination with the linker and the top 200 probe backbone candidates.
108 These two steps are performed by calling the “SelfDimer” and “UNAFoldRun” functions from the IDT
109 web API. Finally, the algorithm will choose the top 10 candidates for each docking stand with the highest
110 T_m and lowest ΔG for homo-dimer and secondary structure predictions. Once the computations are
111 complete, VARNISH will send an email with a link to an output page containing the 10 top probe
112 candidates and the ordering information for both the probes and their corresponding imager strands.
113
114 *sRNA-PAINT detects cellular sRNAs at single molecule resolution*
115 Figure 2a shows the general pipeline for sRNA-PAINT. First, the samples are fixed, embedded in paraffin,
116 and sectioned. Then, thin sections were layered onto coverslips with gold fiducials sealed with silicon
117 dioxide (SiO_2); for this step, we highly recommend that no additional coatings are added, such as poly-l-
118 lysine, since they resulted in non-specific binding. Next, during the hybridization process, probes are
119 applied to fixed and sectioned samples (Fig. 2a). Excess probes are washed off in the washing process.
120 Afterward, imager strands are perfused in. When the un-annealled imager strands drift within the
121 buffer, the speed of the movement is too fast to be caught on by the microscope. However, when an
122 imager strand finds its docking partner, and dwells on it, the short time period before the imager strand
123 dissociates from the docking creates a blinking event that can be detected using a super-resolution
124 microscope. As a result, when thousands of these blinks events are collected, detection of all the
125 docking sites within the sample is eventually completed, defining the locations of the sRNA targets.
126
127 For sRNA-PAINT probe labeling, we evaluated Alexa Fluor® 647 (AF 647), ATTO 665, and ATTO 488. The
128 AF647 dye resulted in the lowest levels of background binding in the negative control samples, whereas

129 ATTO 665 bound to paraffin-embedded plant tissue non-specifically, and ATTO 488 dye emission
130 wavelength overlaps with the strong autofluorescence that is typical of paraffin embedded plant tissue –
131 thus we selected AF674 as the best label (data not shown). The sRNA probes designed by VARNISH were
132 hybridized and the coverslip was mounted in perfusion chamber. The corresponding, 3'-dye-labeled
133 imager strands were continuously perfused and imaging was conducted using total internal reflection
134 fluorescence (TIRF) microscopy. As a demonstration, we performed sRNA-PAINT on an abundant 24-nt
135 phasiRNA – a class of plant secondary siRNAs abundant in the early developmental stages of maize
136 anthers [7] (Fig. 1b); the 24-nt phasiRNAs are triggered by a miRNA, miR2275, providing us with two
137 different classes of small RNAs in one tissue. After the 1st round of imaging, buffer was perfused into the
138 imaging chamber, and the signal was diminished rapidly within 1 min, suggesting that stripping off the
139 imager strand is very efficient. And then, sRNA-PAINT signal was re-achieved by re-applying the imager
140 strands (Fig. 1a, b). Different imager strands had no or very little non-specific binding, which is similar to
141 the original DNA-PAINT method [23]. The scrambled, control probe detected very little to no background
142 (Supplementary Figure 1), which showed that the imager strand does not bind non-specifically to the
143 plant tissue we used. Our sRNA-PAINT experiment was consistent with our previous findings that the 24-
144 nt phasiRNA was present in all of the anther cell layers, and most abundant in the tapetum layer and
145 pollen mother cells [7]; however, our, sRNA-PAINT approach achieved a much higher resolution of below
146 10 nm (Fig. 1 c).
147
148 *Calculation of sRNA copy number with qPAINT*
149 qPAINT can count molecules by analyzing the predictable and programmable binding kinetics of the
150 imager strand to the docking strand [22]. This quantitative method is based solely on binding kinetics, and
151 therefore, individual molecules do not need to be resolved. Picasso software is publicly available and
152 can perform this calculation for the binding sites within a selected region [21]. We selected a 3.18 µm (20
153 pixel) diameter circle in the cytoplasm to represent the copy number in the cytoplasmic region of each
154 cell in each layer, and we performed qPAINT using the same image in Figure 2b. After the count, we
155 calculated the number of binding sites in 63.25 μm^2, which is roughly the area of the cytoplasm of cells
156 in our sections. As shown in Figure 3, we detected 10.41 copies of 24-nt phasiRNA per selected region
157 per cell in epidermal cells, 11.04 copies in endothecial cells, 22.64 copies in middle layer cells, 72.68
158 copies in pollen mother cells, and most abundantly, 61.05 copies in tapetal cells. Pollen mother cells and
159 tapetum have a greater abundance of the 24-nt phasiRNA compared with the other cell layers. qPAINT,
160 in combination with sRNA-PAINT, allowed the detection of the exact copy number of sRNAs in cell

161 sections and the relative sRNA targets in the different cell layers. These data will be useful to ground-
162 truth sequencing data, currently the predominant method of measuring sRNA.
163
164 *Detection of miRNA and phasiRNA with sRNA-Exchange-PAINT*
165 Sequential detection of sRNAs can be done by multiplex VARNISH probes with different docking strand
166 combinations. We name this technique sRNA-Exchange-PAINT, as a variation of the protein-focused,
167 multiplexed Exchange-PAINT method. For this analysis, we measured both miR2275 and the most
168 abundant 24-nt phasiRNA it triggers, again in maize anthers. As shown in the Figure 2b, the imager
169 strand used for miR2275 (P0*) and 24-nt phasiRNA (P1*) do not non-specifically bind to each other's
170 docking strand. Fixed sample were first perfused with P0* imager strand. After the image of miR2275
171 was acquired, buffer wash was performed to completely remove the P0* imager strand. And then
172 imager strand P1* was applied, and generated the image for 24-nt phasiRNA. Using traditional *in situ*
173 hybridization methods, miR2275 and 24-nt phasiRNA were thought to co-localize to each other in the
174 tapetum layer and pollen mother cells. Using sRNA-PAINT, which has the resolution limit down to 10
175 nm, we confirmed that they both localize to the tapetum layer and pollen mother cells (Fig. 4 B), but our
176 results show that they do not co-localize at the single molecule level (Supplementary Fig. 2).
177
178 **Discussion**
179 sRNA-PAINT provides a robust method that quantitatively detects small RNAs with single-molecule
180 resolution. It greatly improves the resolution and precision of sRNA localization compared to other FISH
181 methods, namely those that are limited by the diffraction limit of light. Quantification via dSTORM is
182 hindered by photobleaching that results in an underestimation of the targets, particularly, sRNAs [20]. The
183 small size of sRNAs are generally only detected by one fluorophore per sRNA, as a result, each dye play
184 an important role in terms of quantification. In contrast to other super-resolution methods, such as SR-
185 SIM and dSTORM, absolute quantification of binding sites can be deduced from the known binding
186 kinetics of the imager strands to the docking strands with sRNA-PAINT. Another benefit of using sRNA-
187 PAINT is that it takes less time than regular *in situ* hybridization methods, since it by-passes the antibody
188 incubation and amplification steps that typify those methods. Samples are directly imaged after
189 hybridization and washing, bringing the sample preparation time down from 4 days to overnight. The
190 signal amplification of sRNA-PAINT occurs at the same time as image acquisition, although the time of
191 image acquisition for sRNA-PAINT is longer than traditional sRNA-FISH methods due to the need to take
192 thousands of images for one field of view for detection. Another benefit of bypassing the antibody

193 amplification steps of traditional *in situ* techniques is that the primary and secondary antibodies add
194 significant amount of bulk, decreasing the precision of localization by 24 - 30 nm [26]. Similarly, our simple,
195 single-oligo VARNISH probe design does not require biotin and streptavidin like the original DNA-PAINT
196 method. The primary drawback to sRNA-PAINT is simply the cost of the LNA oligos, which makes it
197 expensive for new probes, although this cost is amortized if the probe is used for many samples, as a
198 typical yield for a purchased LNA oligo is enough for innumerable sRNA-PAINT experiments.
199
200 With the ability to count the exact copy number, this method could be used to investigate many
201 biological questions that require precise subcellular localization or quantitative data, from small RNA
202 biogenesis to the function of sRNAs. Images acquired with sRNA-PAINT may even change the way we
203 consider sRNA localization. The size of a small RNA is about 10 nm [27] and the imaging resolution of our
204 sRNA-PAINT is sub-10 nm. Colocalization of sRNA-PAINT should be evaluated in the context of spatial
205 information at the tissue, subcellular and molecular level. In case of miR2275 and the 24-nt phasiRNA,
206 *in situ* hybridization of these two sRNAs showed that these two co-localize at tissue level in tapetal layer
207 and pollen mother cells, and, at the subcellular level mainly in the cytoplasm. However, at the molecular
208 level, we observed minimal colocalization because sRNA-PAINT has single molecule resolution. Co-
209 localization of miR2275 and its phasiRNA at the molecular level would suggest that they physically
210 interact with each other or that their density is too high for the method to resolve individual target sRNA
211 molecules. Future plan includes generating an analysis pipeline for sRNA-PAINT co-localization that will
212 be most useful for sRNA-mRNA and sRNA-protein interactions, to examine outstanding questions in
213 sRNA biogenesis and processing.
214
215 A distinct advantage of sRNA-PAINT is that it is compatible with Exchange-PAINT, for multiplexing using
216 multiple docking strands that are linked to of the same fluorophore [23]. Our previously describe sRNA-
217 FISH [20] is limited to only 2-3 targets, mainly due to the limited choices of antibody-based amplification
218 and fluorophore choice. sRNA-PAINT only requires the use of single fluorophore and therefore it is not
219 prone to differences in photophysical properties of different flourophores for different targets. Our
220 antibody-free method potentially can be massively multiplexed using numerous probes designed via
221 VARNISH to query many targets in the same sample. The Exchange-PAINT for protein targets predicts
222 that there should be hundreds of non-interacting docking sequences for multiplexing [23], and our sRNA-
223 Exchange-PAINT should have similar multiplexing potential.
224

225 Finally, our sRNA-PAINT method provides an alternative to conventional sRNA-FISH, as it is capable of
226 higher resolution, quantification, and multiplexing. All FISH-based methods are dependent on the actual
227 hybridization efficiency of the probes prior to imaging. The development of LNA technology increased
228 the specificity and efficiency of sRNA-FISH methods; future improvements in probes may provide
229 thorough yet specific labeling of target sRNAs that will benefit all FISH-based RNA detection methods,
230 including sRNA-PAINT. One strategy for increasing specificity is to use a split probe for detection of one
231 sRNA, such that each probe backbone will be 9-10 nt in length. By combining signals from both probe,
232 specific signal could be obtained for each target. Another drawback of the sRNA-PAINT method is that it
233 can only applied to fixed tissues or cells. Live-cell imaging, especially aptamer-based sensor imaging for
234 small RNAs, was made possible by fluorescent RNA aptamers such as Spinach and Mango [28-30]. Creating a
235 live-cell, single-molecule level of sRNA-PAINT would shed light on the dynamics and ever changing
236 contents of cellular RNAs.
237
238 **Methods**
239 *Plant materials and oligonucleotides.*
240 Maize anthers from W23 were provided by the Walbot lab at Stanford University (Palo Alto, CA). Plants
241 were grown in Palo Alto, CA under greenhouse conditions. Anther dissection and measurements were
242 performed as previously described [31]. LNA-modified oligonucleotide probes were designed using our
243 VARNISH software and synthesized by Exiqon (QIAGEN; Germantown, MD). Imager strands coupled with
244 AF647 were ordered from IDT (Coralville, Iowa).
245
246 *Sample preparation.*
247 Sample preparation for *in situ* hybridization was performed as previously described [20]. Briefly, anthers
248 were dissected and fixed in a 50 ml tube using 4% paraformaldehyde in 1xPHEM buffer (5 mM HEPES, 60
249 mM PIPES, 10 mM EGTA, 2 mM $MgSO_4$ at pH 7). Samples were then processed in a vacuum chamber
250 (0.08 MPa) three times, 15 min each. After fixation, samples were embedded in paraffin at the
251 Histochemistry and Tissue Processing Core Lab at Nemours/Alfred I. duPont Hospital for Children
252 (Wilmington, DE). Paraffin samples were sectioned at 6 µm thickness using a paraffin microtome and
253 dried on a Wide Spectral Band 600+/- 100 nm Gold Fiducials coverglass (600-100AuF; Hestzig LLC,
254 Leesburg, VA) at 37° C degree on a slider warmer.
255
256 In situ *hybridization.*

257 The *in situ* hybridization step was performed following our previously-published protocol [20]. Briefly,
258 samples were de-paraffinized using Histo-Clear (item 50-899-90147; Fisher Scientific, Pittsburgh, PA) and
259 re-hydrated by going through an ethanol series of 95, 80, 70, 50, 30, 10% (vol/vol) and water (1 min) at
260 room temperature. Then samples were treated with protease (item P5147; Sigma-Aldrich, St. Louis, MO)
261 for 20 min at 37°C. Excess formaldehyde background was removed by treating samples with 0.2%
262 glycine (item G8898; Sigma-Aldrich) for 20 min. After two washes in 1xPBS buffer (phosphate-buffered
263 saline), samples were de-hydrated by going through an ethanol series of 10, 30, 50, 70, 80, 95%, and
264 100% (vol/vol). Hybridization was done with 10 uM probe at 53.3°C in a hybridization oven. After
265 hybridization, samples were washed twice with 0.2x SSC buffer (saline-sodium citrate). Sample were
266 then washed in 1x BPS buffer for 10 min. Hybridized samples can be kept in 1xPBS at 4°C until imaging.
267
268 *Super-resolution optical.*
269 Super-resolution imaging was carried out on an inverted Zeiss Elyra PS.1 super-resolution microscope
270 (Carl Zeiss, Lberkochen, Germany). TIRF illumination was done using a 100% 642 nm laser and α-Plan-
271 Apochromat 100x/1.46 oil objective. For each imager strand, as well as control imager strand, images
272 were taken with an exposure time of 100 ms, an EMCCD Gain 30, and 20,000 frames in total.
273
274 *PAINT.*
275 A DH40iL culture dish incubate system (model 640388; Warner Instruments LLC, Hamden, CT) and a
276 quick release magnetic chamber for 25 mm low profile, round coverslips (model 641943; Warner
277 Instruments LLC) were assembled to be used as the perfusion chamber. A ValveLink8.2 Perfusion System
278 (AutoMate Scientific, Berkeley, CA) was used for perfusing buffer and imager strand solutions into the
279 chamber. All imager strands were diluted to 0.5-2 nM in buffer C (1× PBS, 500 mM NaCl, pH 8). Imagers
280 were taken with constant flow of imager stand. A Masterflex C/L peristaltic pump (60 RPM, model
281 77120-62; Cole-Parmer Instrument Company LLC, Vernon Hills, IL) was used to collect the buffer flow.
282
283 *Super-resolution image reconstruction.*
284 Each image was analyzed in Zen software (Carl Zeiss). The images were processed using the same
285 parameters, which are listed below: Ignore overlapping molecules; Peak Mask Size (6); Peak Intensity to
286 Noise (6.0); Fit model (x,y 2D Gauss Fit). Drift correction was done by using fiducial-based algorithm. For
287 image rendering, pixel resolution was set to 16 nm/pixel and 2 nm/pixel for zoomed in images with 1x
288 PSF (point spread function) expansion factor.

qPAINT data analysis.

qPAINT data analysis was done following the protocol by Schnitzbauer et al. [21] using the Picasso software package. In brief, 8000 fames of the raw movie file of PAINT data were processed with "Picasso: Localize". We adjusted the threshold until only the PAINT spots were detected and selected. After "Localize (Identify & Fit)", a .hdf5 file was generated and this was used as the input for the next module. The .hdf5 file was opened in "Picasso: Render", and marker-based drift correction or redundant cross-correlative drift correction was performed. A 20 pixel diameter region of interest in the cytoplasm of each anther cell layer was picked by using "Tools: Pick". The dark time under "View: Show info" was used as the input for calculating the influx rate via $\xi = k_{on} \times c$, and the influx rate was used to calculate the copy number.

sRNA sequences.

All small RNA probe sequences and imager strands used are listed below, designing an LNA nucleotide after the "+", the lowercase nucleotides indicate the linker, and the docking strand is underscored:

Scrambled control probe with P0 docking strand:

GTG+T+AA+CACG+T+C+T+A+TACGCCCAtattcgat<u>TTTCAATGTAT</u>

miR2275: TTCAGTTTCCTCTAATATCTCA

Probe for miR2275 with linker and P0 docking strand:

T+GA+GA+TAT+TA+GAG+GAAA+C+TGAAtattcgat<u>TTTCAATGTAT</u>

P0* imager strand: 5'-CATACATTGA-AF647

24 nt-phasiRNA: AGTTGTTGGACCGGACCTTGGCCC

Probe for 24-nt phasiRNA with linker and P1 docking strand:

GGC+C+AAG+G+TC+C+GGTCCA+A+CAACTtattcgat<u>TTATACATCTA</u>

P1* imager strand: 5'-CTAGATGTAT-AF647

Acknowledgements

This project was supported by the US NSF Plant Genome Research Program, awards 1649424, 1611853 and 1754097. We thank members of the Meyers and Caplan labs for help and support. We thank Virginia Walbot (Stanford University) and members of her lab for supplying maize materials and for useful discussions on anther small RNAs. We thank Prof. Dr. Ralf Jungmann for his support in DNA-PAINT, qPAINT and analysis with Picasso. Microscopy equipment was acquired with a shared

instrumentation grant (S10 OD016361) and access was supported by the NIH-NIGMS (P20 GM103446), the NSF (IIA-1301765) and the State of Delaware.

References

1. Lewsey, M.G. et al. Mobile small RNAs regulate genome-wide DNA methylation. *Proc Natl Acad Sci U S A* **113**, E801-810 (2016).
2. Baldrich, P. et al. Plant Extracellular Vesicles Contain Diverse Small RNA Species and Are Enriched in 10-to 17-Nucleotide "Tiny" RNAs. *Plant Cell* **31**, 315-324 (2019).
3. Wight, C., Ross, D.A. & Weinberger, D.R. Small RNAs May Answer Big Questions in Mental Illness. *Biological Psychiatry* **83**, E1-E3 (2018).
4. Borges, F. & Martienssen, R.A. The expanding world of small RNAs in plants. *Nature Reviews Molecular Cell Biology* **16**, 727-741 (2015).
5. Fei, Q., Xia, R. & Meyers, B.C. Phased, secondary, small interfering RNAs in posttranscriptional regulatory networks. *Plant Cell* **25**, 2400-2415 (2013).
6. Xia, R. et al. 24-nt reproductive phasiRNAs are broadly present in angiosperms. *Nature Communications* **10** (2019).
7. Zhai, J.X. et al. Spatiotemporally dynamic, cell-type-dependent premeiotic and meiotic phasiRNAs in maize anthers. *P Natl Acad Sci USA* **112**, 3146-3151 (2015).
8. Chitwood, D.H. & Timmermans, M.C.P. Small RNAs are on the move. *Nature* **467**, 415-419 (2010).
9. Fang, Y.D. & Spector, D.L. Identification of nuclear dicing bodies containing proteins for microRNA biogenesis in living Arabidopsis plants. *Current Biology* **17**, 818-823 (2007).
10. Li, C.F. et al. An ARGONAUTE4-containing nuclear processing center colocalized with Cajal bodies in Arabidopsis thaliana. *Cell* **126**, 93-106 (2006).
11. Li, S.B. et al. Biogenesis of phased siRNAs on membrane-bound polysomes in Arabidopsis. *Elife* **5** (2016).
12. Song, L., Han, M.H., Lesicka, J. & Fedoroff, N. Arabidopsis primary microRNA processing proteins HYL1 and DCL1 define a nuclear body distinct from the Cajal body. *P Natl Acad Sci USA* **104**, 5437-5442 (2007).
13. Dunoyer, P., Melnyk, C., Molnar, A. & Slotkin, R.K. Plant Mobile Small RNAs. *Cold Spring Harbor Perspectives in Biology* **5** (2013).
14. Yoo, B.C. et al. A systemic small RNA signaling system in plants. *Plant Cell* **16**, 1979-2000 (2004).
15. Johnson, N.R. & Axtell, M.J. Small RNA warfare: exploring origins and function of trans-species microRNAs from the parasitic plant Cuscuta. *Curr Opin Plant Biol* **50**, 76-81 (2019).
16. Cai, Q. et al. Plants send small RNAs in extracellular vesicles to fungal pathogen to silence virulence genes. *Science* **360**, 1126-1129 (2018).
17. Liu, T. et al. EVmiRNA: a database of miRNA profiling in extracellular vesicles. *Nucleic Acids Research* **47**, D89-D93 (2019).
18. Javelle, M. & Timmermans, M.C.P. In situ localization of small RNAs in plants by using LNA probes. *Nature Protocols* **7**, 533-541 (2012).
19. Hell, S.W. Microscopy and its focal switch. *Nature Methods* **6**, 24-32 (2009).
20. Huang, K., Baldrich, P., Meyers, B.C. & Caplan, J.L. sRNA-FISH: versatile fluorescent in situ detection of small RNAs in plants. *Plant Journal* **98**, 359-369 (2019).
21. Schnitzbauer, J., Strauss, M.T., Schlichthaerle, T., Schueder, F. & Jungmann, R. Super-resolution microscopy with DNA-PAINT. *Nature Protocols* **12**, 1198-1228 (2017).
22. Jungmann, R. et al. Quantitative super-resolution imaging with qPAINT. *Nature Methods* **13**, 439-442 (2016).
23. Jungmann, R. et al. Multiplexed 3D cellular super-resolution imaging with DNA-PAINT and Exchange-PAINT. *Nature Methods* **11**, 313-318 (2014).

370 24. Xu, W.D., Yin, P. & Dai, M.J. Super-resolution Geometric Barcoding for Multiplexed miRNA
371 Profiling. *Angewandte Chemie-International Edition* **57**, 14075-14079 (2018).
372 25. McTigue, P.M., Peterson, R.J. & Kahn, J.D. Sequence-dependent thermodynamic parameters; for
373 locked nucleic acid (LNA)-DNA duplex formation. *Biochemistry* **43**, 5388-5405 (2004).
374 26. Pleiner, T. et al. Nanobodies: site-specific labeling for super-resolution imaging, rapid epitope-
375 mapping and native protein complex isolation. *Elife* **4** (2015).
376 27. Yoffe, A.M. et al. Predicting the sizes of large RNA molecules. *P Natl Acad Sci USA* **105**, 16153-
377 16158 (2008).
378 28. Autour, A. et al. Fluorogenic RNA Mango aptamers for imaging small non-coding RNAs in
379 mammalian cells. *Nature Communications* **9** (2018).
380 29. Huang, K. et al. FASTmiR: an RNA-based sensor for in vitro quantification and live-cell
381 localization of small RNAs. *Nucleic Acids Research* **45** (2017).
382 30. Paige, J.S., Wu, K.Y. & Jaffrey, S.R. RNA Mimics of Green Fluorescent Protein. *Science* **333**, 642-
383 646 (2011).
384 31. Kelliher, T. & Walbot, V. Emergence and patterning of the five cell types of the *Zea mays* anther
385 locule. *Dev Biol* **350**, 32-49 (2011).
386
387

388 **Figure legends**

389 *Figure 1. Illustration of an sRNA-PAINT probe.*

390 An sRNA-PAINT probe is composed of three parts: a probe backbone (cyan) that is complementary to
391 the target sRNA (orange), a docking strand (green) and a linker sequence (dark blue) connecting them.
392 The imager strand is conjugated to the fluorophore, and it will find its corresponding docking strand
393 during the imaging process.

394

395 *Figure 2. sRNA-PAINT on a 24 nt-phasiRNA in an early-stage maize anther.*

396 **a.** A work flow of sRNA-PAINT. Sample were fixed and embedded, and a thin section is placed on the
397 coverglass. During the hybridization process, the VARNISH probes will bind to sRNAs in the sample. **b.** an
398 example of the sRNA-PAINT imaging process. In the first imaging step, imager strands are added to the
399 probe-hybridized sample on the coverglass. After the image is acquired, the imager strands are washed
400 off with a short buffer wash step. In the second imaging step, the signal can be re-detected when re-
401 applying the imager strand to the sample. A non-specific imager stand was used as a negative control. **c.**
402 Detection of a 24-nt phasiRNA in a cross-section of maize anther. The sRNA-PAINT signal was detected in
403 all cell layers but it is most abundant in the tapetal layer and pollen mother cells. **c.** Zoomed images of
404 boxes 1 and 2 in panel b. There are more 24-nt phasiRNA localization events in the pollen mother cells
405 (box 1) compared to the epidermal and endothecium layers (box 2). The dotted line (light blue) marks
406 the division between the epidermal (above the line) and endothecium layers (below the line). Expanded
407 boxed areas (white) show representative areas at higher magnification. A red-to-white lookup table was
408 used to display low-to-high intensity values.

409

410 *Figure 3. Quantification of binding site per cell in each layer.*

411 Cartoon diagram representing each cell layer of a cross section of a maize anther lobe: epidermis
412 (yellow), endothecium (green), middle layer (red), tapetum (blue), and pollen mother cells (purple). The
413 Picasso software was used to calculate the binding sites by choosing a region of interest in the
414 cytoplasmic area of each cell layer. 10.41, 22.64, 72.68 and 61.05 copies of 24-nt phasiRNA per selected
415 region per cell in epidermal cells, endothecial cells, middle layer cells, and pollen mother cells
416 respectively.

417

418 *Figure 4. sRNA-Exchange-PAINT*

419 **a.** A diagram showing sRNA-Exchange-PAINT, which differs from sRNA-PAINT via the use of multiple
420 imager strands. Imager strand 1 is first introduced to the sample, and after imaging, imager strand 1 is
421 removed with a buffer wash. Next, imager strand 2 is introduced. This process can be repeated until the
422 needed number of targets is reached. **b.** sRNA-Exchange-PAINT on miR2275 (yellow) and a 24-nt
423 phasiRNA (blue) in maize anther. After the buffer wash, imaging showed little or no signal following each
424 round of detection using the imager strands. Scale bar = 10 µm for all images.
425
426
427 **Supplemental figure legends**
428 *Supplementary Figure 1. sRNA-PAINT showed limited to no background with a scrambled control probe.*
429 **a.** sRNA-PAINT with probes for a 24-nt phasiRNA and a scrambled control. Both docking strands were
430 detected with corresponding imager strands. Arrows indicate 2 out of ~66 fiducials used in experiments.
431 Scrambled control detected little or no signal. Scale bar = 10 µm for all images. **b.** qPAINT analysis of
432 image in panel a. Number showed the binding events for each cell (80 pixel size diameter circle in
433 Picasso software) in different cell layers.
434
435 *Supplementary Figure 2. Subcellular localization analysis of miR2275 and 24-nt phasiRNA in maize*
436 *anther.*
437 Right panel: zoomed image of the marked region in the left panel. These two sRNAs do not co-localize at
438 a nanometer resolution.

Fig 1.

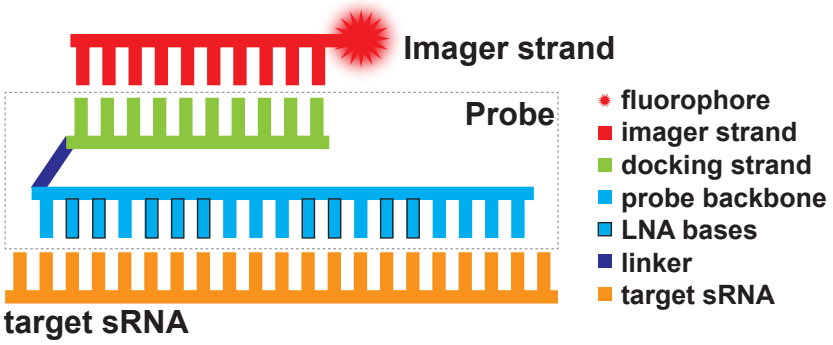

Figure 1. Illustration of an sRNA-PAINT probe.
An sRNA-PAINT probe is composed of three parts: a probe backbone (cyan) that is complementary to the target sRNA (orange), a docking strand (green) and a linker sequence (dark blue) connecting them. The imager strand is conjugated to the fluorophore, and it will find its corresponding docking strand during the imaging process.

Fig. 2

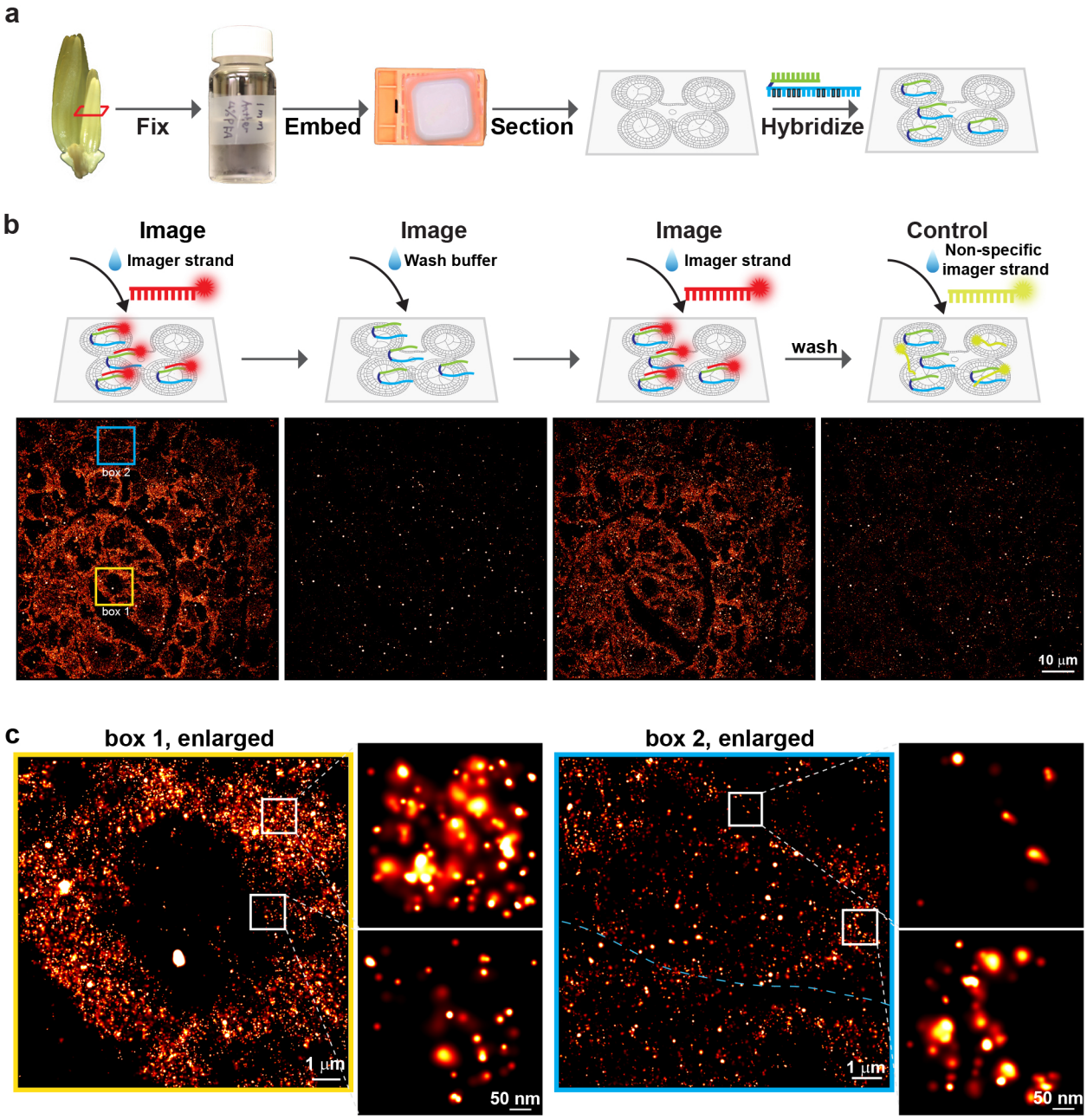

Figure 2. sRNA-PAINT on a 24 nt-phasiRNA in an early-stage maize anther.
a. A work flow of sRNA-PAINT. Sample were fixed and embedded, and a thin section is placed on the coverglass. During the hybridization process, the VARNISH probes will bind to sRNAs in the sample. b. an example of the sRNA-PAINT imaging process. In the first imaging step, imager strands are added to the probe-hybridized sample on the coverglass. After the image is acquired, the imager strands are washed off with a short buffer wash step. In the second imaging step, the signal can be re-detected when re-applying the imager strand to the sample. A non-specific imager stand was used as a negative control. c. Detection of a 24-nt phasiRNA in a cross-section of maize anther. The sRNA-PAINT signal was detected in all cell layers but it is most abundant in the tapetal layer and pollen mother cells. c. Zoomed images of boxes 1 and 2 in panel b. There are more 24-nt phasiRNA localization events in the pollen mother cells (box 1) compared to the epidermal and endothecium layers (box 2). The dotted line (light blue) marks the division between the epidermal (above the line) and endothecium layers (below the line). Expanded boxed areas (white) show representative areas at higher magnification. A red-to-white lookup table was used to display low-to-high intensity values.

Fig.3

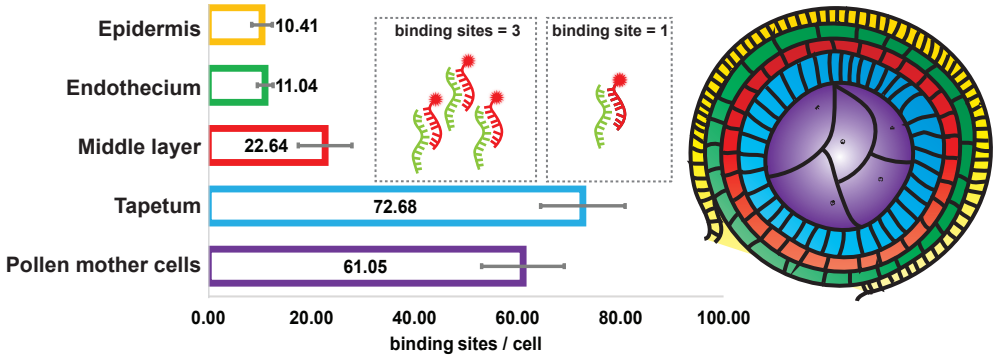

Figure 3. Quantification of binding site per cell in each layer.
Cartoon diagram representing each cell layer of a cross section of a maize anther lobe: epidermis (yellow), endothecium (green), middle layer (red), tapetum (blue), and pollen mother cells (purple). The Picasso software was used to calculate the binding sites by choosing a region of interest in the cytoplasmic area of each cell layer. 10.41, 22.64, 72.68 and 61.05 copies of 24-nt phasiRNA per selected region per cell in epidermal cells, endothecial cells, middle layer cells, and pollen mother cells respectively.

Fig.4

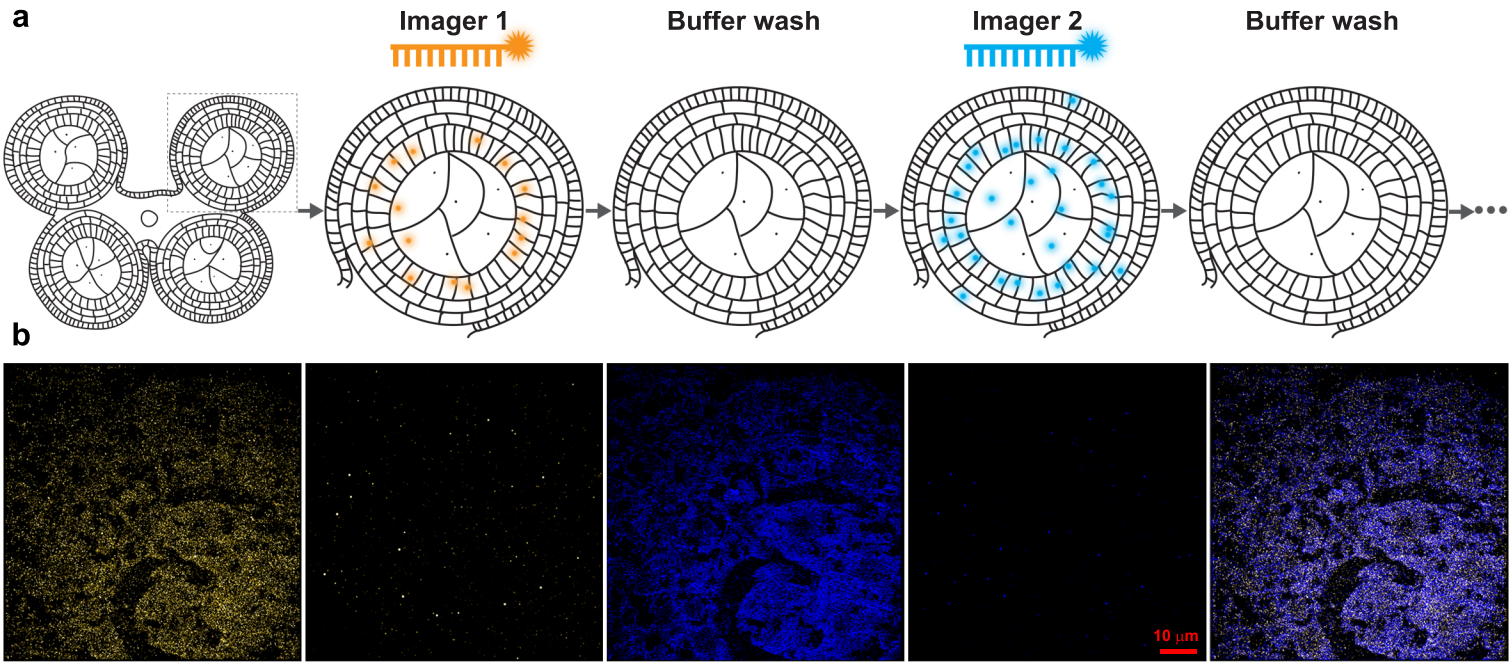

Figure 4. sRNA-Exchange-PAINT
a. A diagram showing sRNA-Exchange-PAINT, which differs from sRNA-PAINT via the use of multiple imager strands. Imager strand 1 is first introduced to the sample, and after imaging, imager strand 1 is removed with a buffer wash. Next, imager strand 2 is introduced. This process can be repeated until the needed number of targets is reached. b. sRNA-Exchange-PAINT on miR2275 (yellow) and a 24-nt phasiRNA (blue) in maize anther. After the buffer wash, imaging showed little or no signal following each round of detection using the imager strands. Scale bar = 10 μm for all images.

Supplementary Fig. 1

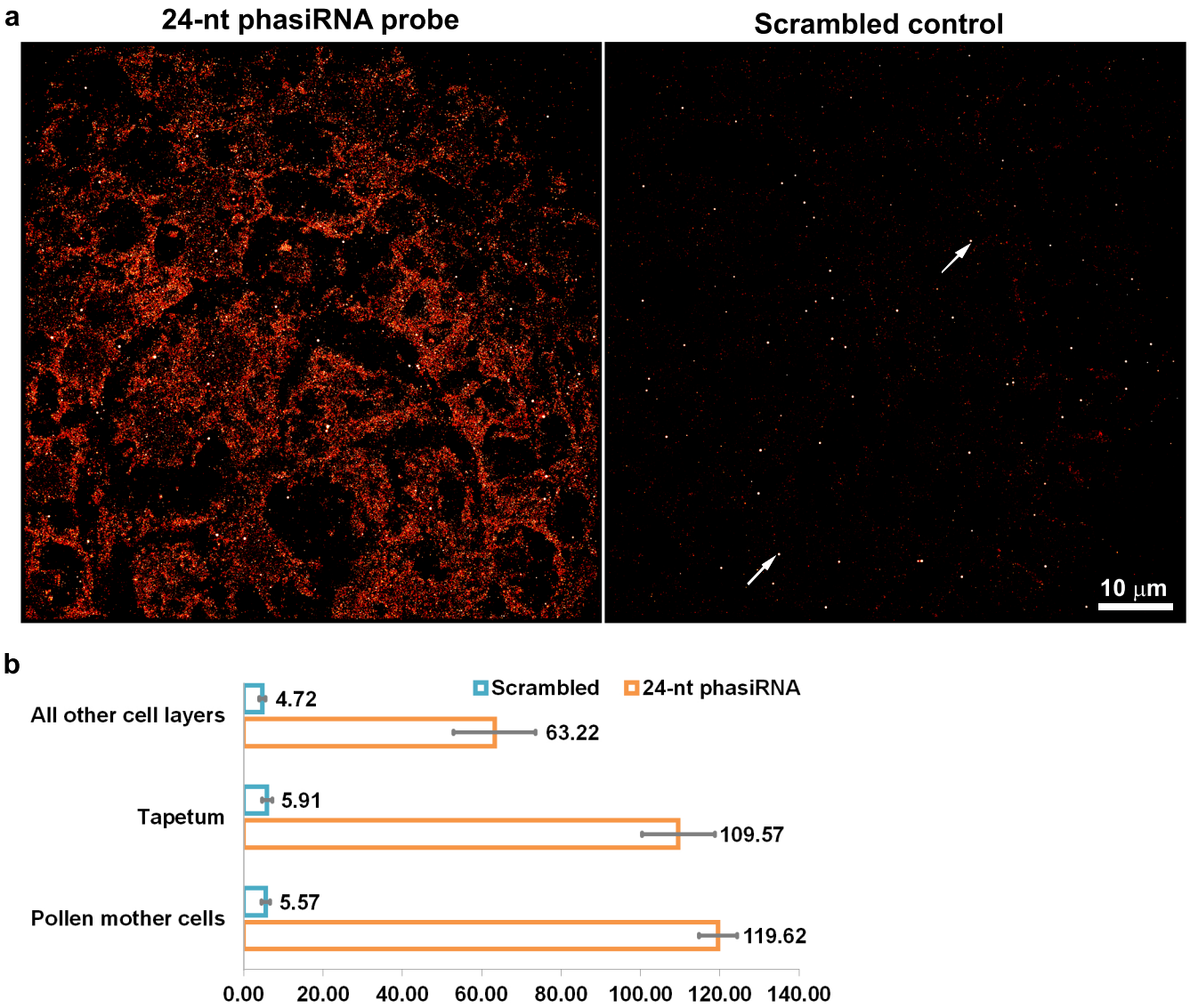

Supplementary Figure 1. sRNA-PAINT showed limited to no background with a scrambled control probe.
a. sRNA-PAINT with probes for a 24-nt phasiRNA and a scrambled control. Both docking strands were detected with corresponding imager strands. Arrows indicate 2 out of ~66 fiducials used in experiments. Scrambled control detected little or no signal. Scale bar = 10 μm for all images. b. qPAINT analysis of image in panel a. Number showed the binding events for each cell (80 pixel size diameter circle in Picasso software) in different cell layers.

Supplementary Fig. 2

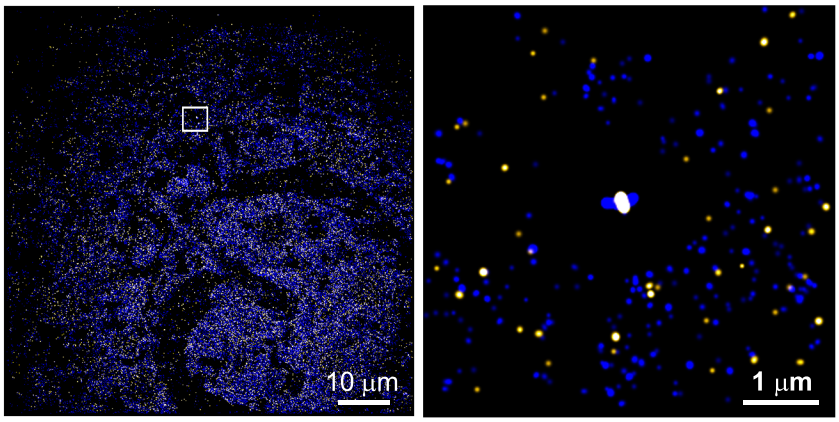

Supplementary Figure 2. Subcellular localization analysis of miR2275 and 24-nt phasiRNA in maize anther. Right panel: zoomed image of the marked region in the left panel. These two sRNAs do not co-localize at a nanometer resolution.